Journal of Solid State Chemistry 182 (2009) 855–861

Contents lists available at ScienceDirect

Journal of Solid State Chemistry

journal homepage: www.elsevier.com/locate/jssc

Synthesis, crystal structure and optical properties of an indium phosphate $K_3In_3P_4O_{16}$

S.-L. Yang, H. Zhang, Z. Xie, D. Zhao, W.-L. Zhang, W.-D. Cheng *

State Key Laboratory of Structural Chemistry, Fujian Institute of Research on the Structure of Matter, Chinese Academy of Sciences, Fuzhou, Fujian 350002, China

ARTICLE INFO

Article history:
Received 6 October 2008
Received in revised form
12 January 2009
Accepted 14 January 2009
Available online 21 January 2009

Keywords:
Indium phosphate
Crystal structure
Band structure
Optical properties
Two-photon absorption

ABSTRACT

An alkali-metal indium phosphate crystal, $K_3In_3P_4O_{16}$, has been synthesized by a high-temperature solution reaction and exhibits a new structure in the family of the alkali-metal indium phosphates system. Single-crystal X-ray diffraction analysis shows the structure to be monoclinic with space group $P2_1/n$, and the following cell parameters: $a = 9.7003(18)$, $b = 9.8065(18)$, $c = 15.855(3)$ Å, $\beta = 90.346(3)^\circ$, $V = 1508.2(5)$ Å^3, $Z = 4$, $R = 0.0254$. It possesses three-dimensional $[In_3(PO_4)_4]_n^{3-}$ anionic frameworks with tunnels occupied by K^+ cations running along the *a*-axis. The emission and absorption spectra of the compound have been investigated. Additionally, the calculations of energy band structure, density of states, dielectric constants and refractive indexes have been performed with the density functional theory method. Also, the two-photon absorption spectrum is simulated by two-band model. The obtained results tend to support the experimental data.

1. Introduction

At present, metal phosphates have attracted extensive attention because of the diversity of the P_nO_m groups, which contain not only the isolated PO_4 [1–3] but also various of other groups, such as P_2O_7 [4–6], P_3O_{10} [7], P_3O_9 [8], P_4O_{12} [9], P_6O_{18} [10] and so on. Furthermore, metal phosphates have shown a rich structural chemistry and optical and chemical properties [11–13]. Among a large number of existing alkali-metal phosphates, only two belong to the K_2O–In_2O_3–P_2O_5 pseudo-ternary system: $KInP_2O_7$ [14] and $K_3InP_2O_8$ [15,16]. $KInP_2O_7$ crystallizes in monoclinic system with space group $P2_1/c$ and possesses three-dimensional $(InP_2O_7)^-$ anionic frameworks with channels occupied by K^+ cations. $K_3InP_2O_8$ also belongs to the monoclinic system but has two different structure, Arakcheeva et al. [15] showed that $K_3In(PO_4)_2$ has the incommensurately modulated structure with (3+1)D superspace group $X2/b(\alpha\beta0)0s$, while Zhang et al. [16] solved the $K_3In(PO_4)_2$ structure in the 3D space group $C2/c$.

In the course of ongoing investigations for the search of new phosphates and their optical properties, we present the synthesis, crystal structure determinations, and spectral measurements for indium phosphate $K_3In_3P_4O_{16}$ in this paper. At the same time, we also make the calculations of crystal energy band structure, density of states (DOS), dielectric constants, and refractive indexes of $K_3In_3P_4O_{16}$ by the density functional theory (DFT) method, as well as simulate the two-photon absorption (TPA) spectrum by two-band model.

2. Experimental section

2.1. Synthesis and characterization

2.1.1. Crystal growth

Single crystals of the title compound were grown by a high-temperature solid-state reaction. All of the chemicals were analytically pure from commercial sources and used without further purification. The reagents were weighted in the molar ratio $KCl/KH_2PO_4/In_2O_3 = 10/6/1$, and the excess of KCl acted as the flux. These starting materials were finely ground in an agate mortar to ensure the best homogeneity and reactivity. The synthesis was performed by two steps. First, the mixture was preheated in a platinum crucible in air at 573 K. Secondly, the products were held at 1073 K for 10 hours, then slowly cooled down to 973 K at a rate of 2 K/h, to 673 K at a rate of 10 K/h, and finally quenched to room temperature. A few colorless crystals were obtained from the melt of the mixture.

2.1.2. Powder preparation

The powder of $K_3In_3P_4O_{16}$ was prepared from the stoichiometric mixture of $NH_4H_2PO_4$, K_2CO_3 and In_2O_3. This mixture was ground in an agate mortar, and then calcined at 873 K in air for 15 hours with several intermediate grindings in an opening Pt

* Corresponding author. Fax: +86 591 83714946.
E-mail addresses: cwd@fjirsm.ac.cn, cwd@ms.fjirsm.ac.cn (W.-D. Cheng).

0022-4596/$ - see front matter © 2009 Elsevier Inc. All rights reserved.
doi:10.1016/j.jssc.2009.01.010

crucible. The final product was analyzed by X-ray powder diffraction.

2.1.3. X-ray powder analysis

In order to check the powder sample used for spectral measurement is a single phase, we refined the structural parameters of $K_3In_3P_4O_{16}$ from the powder X-ray diffraction data in terms of the Rietveld method [17] by using the computer program LHPM-Rietica [18]. The XRD data was collected by PANalytical X'Pert Pro diffractometer with Cu-$K\alpha$ radiation (step size 0.0167° and range 5–85°). Fig. 1 shows the Rietveld refinement results for $K_3In_3P_4O_{16}$ with $R_p = 5.44\%$, $R_{wp} = 6.81\%$ and $R_{exp} = 2.29\%$.

2.2. Spectral measurements

The absorption spectrum was carried on a Perkin-Elmer Lambda 900/UV/Vis/NIR spectrophotometer in the wave length range of 200–800 nm, and the emission spectrum was measured on a FLS920 time-resolved fluorescence spectrometer using a Xe lamp at room temperature.

2.3. Crystal structure determination

X-ray diffraction data of the single-crystal was collected on a Rigaku Mercury CCD diffractometer with graphite-monochromated Mo-$K\alpha$ radiation ($\lambda = 0.71073$ Å) at the temperature of 293 K using the ω/θ scan code. The SHELXL-97 program package [19] was used to determine the structure of $K_3In_3P_4O_{16}$. The cell parameters, data acquisition and structure solution of the crystal are listed in Table 1. All atoms coordinates with the equivalent thermal displacement parameters are listed in Table 2. Tables 3 and 4 give the anisotropic atomic displacement parameters and the selected bond distances . Further details of the crystal structure investigation(s) can be obtained from the Fachinformationszentrum Karlsruhe, 76344 Eggenstein-Leopoldshafen, Germany, (fax: +49 7247 808 666; e-mail: crysdata@fiz.karlsruhe.de) on quoting the depository number CSD 420106.

2.4. Computational details

The crystallographic data of $K_3In_3P_4O_{16}$ determined by X-ray single diffraction was used to calculate its energy band structure. The calculation of the energy band structure was based on the DFT with non-local gradient-correct exchange-correlation function [20] and performed with the CASTEP code [21,22], which uses a plane wave basis set for the valence electrons and norm-conserving pseudopotential [23,24] for the core states. The quality in the setup of the CASTEP code was set to be medium. The number of plane waves included in the basis was determined by a cutoff energy of 450 eV and the numerical integration of the Brillouin zone is performed using a $2 \times 2 \times 1$ Monkhorst-Pack k-point sampling, the self-consistent field (SCF) tolerance is 2.0e−6 eV/atom for $K_3In_3P_4O_{16}$. Pseudoatomic calculations were performed for In-$5s^25p^1$, P-$3s^23p^3$, O-$2s^22p^4$ and K-$3s^23p^64s^1$. The

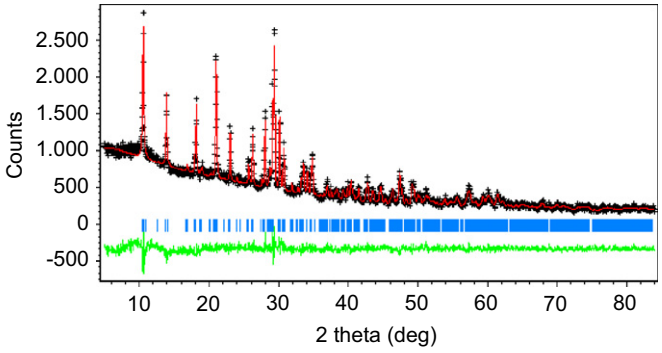

Fig. 1. Final Rietveld refinement patterns for $K_3In_3P_4O_{16}$. Small crosses represent the experimental values and solid lines the calculated pattern. The solid line at the bottom is the difference between the experimental and calculated values. The vertical bars show the positions of the calculated values for the Bragg reflection.

Table 1
Crystal data and structure refinement for $K_3In_3P_4O_{16}$.

Empirical formula	$K_3In_3P_4O_{16}$
Formula weight	841.64 g/mol
Temperature	293(2) K
Wavelength	0.71073 Å
Crystal system, space group	Monoclinic, $P2_1/n$
Unit cell dimensions	$a = 9.7003(18)$ Å $\alpha = 90°$ $b = 9.8065(18)$ Å $\beta = 90.346(3)$º $c = 15.855(3)$ Å $\gamma = 90°$
Volume	1508.2(5) Å^3
Z, calculated density	4, 3.707 mg m^{-3}
Absorption coefficient	5.888 mm^{-1}
$F(000)$	1568
Crystal size	0.20 mm × 0.15 mm × 0.10 mm
Theta range for data collection	2.44–27.48°
Limiting indices	$-12 <= h <= 12$, $-11 <= k <= 12$, $-20 <= l <= 20$
Reflections collected/unique	11043/3436 [R(int) = 0.0261]
Completeness to theta = 25.01	99.4%
Refinement method	Full-matrix least-squares on F^2
Data/restraints/parameters	3436/0/236
Goodness-of-fit on F^2	1.080
Final R indices [$I>2$sigma(I)]	$R1 = 0.0234$, w$R2 = 0.0565$
R indices (all data)	$R1 = 0.0258$, w$R2 = 0.0580$
Largest diff. peak and hole	1.874 and −1.550 e Å^{-3}

$R_1 = \sum ||F_{obc}| - |F_{calc}|| / \sum |Fobs|$
$wR_2 = [\sum w(F_{obs}^2 - F_{calc}^2)^2 / \sum w(F_0^2)]^{1/2}$

Table 2
Atomic coordinates ($\times 10^4$) and equivalent isotropic displacement parameters (Å$^2 \times 10^3$) for $K_3In_3P_4O_{16}$.

Atoms	x	y	z	U(eq)
In1	3234(1)	7716(1)	1353(1)	7(1)
In2	8121(1)	11415(1)	1611(1)	9(1)
In3	7555(1)	9245(1)	9808(1)	7(1)
P4	8665(1)	9687(1)	7884(1)	7(1)
P5	6365(1)	8960(1)	2039(1)	8(1)
P6	9432(1)	12332(1)	46(1)	8(1)
P7	4469(1)	7774(1)	9744(1)	7(1)
O16	8627(3)	12932(3)	9306(2)	13(1)
O15	8899(3)	10876(2)	283(2)	12(1)
O14	4246(3)	6550(2)	341(2)	13(1)
O13	4810(3)	8758(3)	2014(2)	17(1)
O12	3867(3)	8997(2)	270(2)	10(1)
O11	8066(3)	9007(3)	7092(2)	16(1)
O10	8170(3)	8939(3)	8661(2)	18(1)
O9	8121(3)	11157(2)	7872(2)	13(1)
O8	10963(3)	12306(2)	9796(2)	13(1)
O7	3704(3)	7617(2)	8908(2)	13(1)
O6	9216(3)	13110(3)	878(2)	16(1)
O5	6755(3)	10169(3)	2594(2)	20(1)
O4	10243(3)	9722(3)	7842(2)	16(1)
O3	7060(3)	7644(3)	2321(2)	19(1)
O2	6000(3)	7890(3)	9572(2)	19(1)
O1	7012(3)	9389(3)	1187(2)	22(1)
K1	11748(1)	13921(1)	1311(1)	30(1)
K2	8273(1)	10291(1)	3984(1)	41(1)
K3	10235(1)	12733(1)	7848(1)	46(1)

U(eq) is defined as one-third of the trace of the orthogonalized U_{ij} tensor.

Table 3
Anisotropic atomic displacement parameters (Å^2) for $K_3In_3P_4O_{16}$.

Atom	U11	U22	U33	U12	U13	U23
In1	0.00687(13)	0.00676(13)	0.00796(13)	0.00004(9)	−0.00012(9)	0.00121(8)
In2	0.00852(13)	0.00983(13)	0.00845(13)	0.00159(9)	−0.00042(9)	−0.00127(8)
In3	0.00711(13)	0.00624(13)	0.00779(12)	−0.00041(9)	−0.00017(9)	0.00029(8)
P4	0.0076(4)	0.0075(4)	0.0072(4)	0.0006(3)	−0.0003(3)	−0.0018(3)
P5	0.0069(4)	0.0085(4)	0.0091(4)	−0.0005(3)	−0.0003(3)	0.0030(3)
P6	0.0057(4)	0.0092(4)	0.0078(4)	−0.0006(3)	−0.0009(3)	−0.0006(3)
P7	0.0061(4)	0.0078(4)	0.0084(4)	0.0003(3)	−0.0005(3)	−0.0008(3)
O16	0.0093(13)	0.0154(13)	0.0154(13)	−0.0027(10)	−0.0046(10)	0.0032(10)
O15	0.0107(12)	0.0091(12)	0.0158(13)	−0.0032(10)	−0.0013(10)	−0.0008(9)
O14	0.0190(14)	0.0079(11)	0.0133(13)	0.0051(10)	0.0029(11)	0.0013(9)
O13	0.0083(13)	0.0263(15)	0.0168(13)	−0.0072(11)	−0.0031(10)	−0.0036(11)
O12	0.0105(12)	0.0087(11)	0.0094(12)	0.0004(10)	0.0002(9)	−0.0006(9)
O11	0.0246(15)	0.0102(12)	0.0134(13)	0.0039(11)	−0.0070(11)	−0.0049(10)
O10	0.0239(15)	0.0189(14)	0.0096(12)	0.0001(12)	0.0053(11)	0.0024(10)
O9	0.0109(13)	0.0086(12)	0.0186(13)	0.0021(10)	0.002(1)	−0.0037(10)
O8	0.0065(12)	0.0118(12)	0.0193(14)	0.0009(10)	0.0026(10)	0.0037(10)
O7	0.0142(13)	0.0120(12)	0.0112(12)	0.0049(10)	−0.0055(10)	−0.0021(9)
O6	0.0163(13)	0.0169(13)	0.0135(13)	−0.0021(11)	0.0017(10)	−0.0066(10)
O5	0.0183(14)	0.0131(13)	0.0294(16)	−0.0028(11)	−0.0038(12)	−0.0042(11)
O4	0.0077(12)	0.0174(14)	0.0225(14)	0.0034(11)	0.0007(11)	0.0033(11)
O3	0.0229(15)	0.0155(14)	0.0177(14)	0.0075(11)	0.0057(12)	0.0094(11)
O2	0.0079(13)	0.0195(14)	0.0295(16)	−0.0038(11)	0.0049(11)	−0.0111(12)
O1	0.0240(16)	0.0264(16)	0.0162(14)	0.0040(13)	0.0069(12)	0.0075(11)
K1	0.0341(6)	0.0263(5)	0.0294(5)	−0.0102(4)	−0.0140(4)	−0.0057(4)
K2	0.0565(7)	0.0270(5)	0.0409(6)	−0.0034(5)	−0.0276(6)	0.0067(4)

The anisotropic displacement factor exponent takes the form: $-2\pi^2(h^2a^2U_{11}+\cdots+2hkab\,U_{12}+\cdots)$.

Table 4
Selected distances (Å) for $K_3In_3P_4O_{16}$.

Atoms	*d* 1,2	Atoms	*d* 1,2
In1–O11i	2.063(2)	P6–O8	1.540(3)
In1–O13	2.112(3)	P6–O15	1.565(2)
In1–O9ii	2.115(2)	P7–O2	1.516(3)
In1–O16ii	2.174(3)	P7–O7	1.524(3)
In1–O14	2.206(2)	P7–O14	1.544(3)
In1–O12	2.217(2)	P7–O12	1.575(2)
In2–O3v	2.087(3)	K3–O5xv	2.564(3)
In2–O4vi	2.121(3)	K3–O3vi	2.665(3)
In2–O7ii	2.166(3)	K3–O7xvi	2.976(3)
In2–O6	2.294(3)	K3–O9	2.569(3)
In2–O15	2.303(3)	K3–O16	2.803(3)
In2–O1	2.355(3)	K3–O4	2.953(3)
In2–O5	2.388(3)	K3–O8	3.191(3)
In3–O2	2.078(3)	K1–O16x	3.257(3)
In3–O10	2.091(3)	K1–O13v	3.067(3)
In3–O1	2.102(3)	K1–O2vi	3.149(3)
In3–O8vi	2.143(2)	K1–O8	2.973(3)
In3–O15	2.145(2)	K1–O6	2.668(3)
In3–O12ii	2.225(2)	K1–O11xiii	2.697(3)
P4–O10	1.515(3)	K1–O9xiii	2.805(3)
P4–O11	1.533(3)	K1–O10vi	2.807(3)
P4–O4	1.533(3)	K2–O7xiv	2.885(3)
P4–O9	1.535(3)	K2–O14v	2.903(3)
P5–O3	1.521(3)	K2–O14xiv	2.958(3)
P5–O13	1.521(3)	K2–O3v	3.115(3)
P5–O5	1.523(3)	K2–O6iii	3.234(3)
P5–O1	1.552(3)	K2–O4vi	3.241(3)
P6–O16	1.524(3)	K2–O7xiv	2.885(3)
P6–O6	1.539(3)	K2–O5	2.646(3)

Symmetry transformations used to generate equivalent atoms: (i) −0.5+*x*, 1.5−*y*, 0.5+*z*; (ii) 1−*x*, 2−*y*, −*z*; (iii) 1.5−*x*, −0.5+*y*, 0.5−*z*; (iv) −1+*x*, −1+*y*, *z*; (v) 1.5−*x*, 0.5+*y*, 0.5−*z*; (vi) 2−*x*, 2−*y*, −*z*; (vii) −0.5+*x*, 2.5−*y*, 0.5+*z*; (viii) −0.5+*x*, 2.5−*y*, −0.5+*z*; (ix) −0.5+*x*, 1.5−*y*, −0.5+*z*; (x) 2−*x*, 3−*y*, −*z*; (xi) 0.5+*x*, 1.5−*y*, −0.5+*z*; (xii) 1.5−*x*, −0.5+*y*, −0.5−*z*; (xiii) 0.5+*x*, 2.5−*y*, 0.5+*z*; (xiv) 0.5+*x*, 1.5−*y*, 0.5+*z*; (xv) 0.5+*x*, 2.5−*y*, −0.5+*z*; (xvi) 1.5−*x*, 0.5+*y*, −0.5−*z*.

calculations of linear optical properties described in terms of complex dielectric function $\varepsilon(\omega)=\varepsilon_1(\omega)+i\varepsilon_2(\omega)$ were also carried out in this work. CASTEP calculated the real $\varepsilon_1(\omega)$ and imaginary $\varepsilon_2(\omega)$ parts of the dielectric function. The $\varepsilon_2(\omega)$ can be thought of as detailing the real transitions between occupied and unoccupied electronic states. The real and imaginary parts were linked by a Kramers–Kroning transform [25]. This transform was used to obtain the real part $\varepsilon_1(\omega)$ of the dielectric function.

3. Results and discussion

3.1. Structure description

As shown in Fig. 2, the crystal $K_3In_3P_4O_{16}$ possesses three-dimensional $[In_3(PO_4)_4]_n^{3-}$ anionic frameworks built by InO_6 octahedra, InO_7 decahedra and PO_4 tetrahedra. There are three different K cations: K1, K2 and K3. As depicted in Fig. 3, K1 is surrounded by eight O atoms at the distances from 2.668(3) to 3.257(3) Å, while K2 and K3 are coordinated to seven O atoms, and K–O distances of 2.646(3)–3.241(3) Å for K2, 2.564(3)–3.191(3) Å for K3 (Table 4). K1 and K2 are located inside the tunnels with 12-membered ring (Fig. 4), each ring is formed by the edges of two InO_7 octahedra, four InO_6 decahedra and six PO_4 tetrahedra. K3 cations are located in cavities of the structure: from one side along the *a*-axis between InO_6 and InO_7 polyhedra and between two 12-membered ring from another side. Fig. 5 shows the structure of $K_3In_3P_4O_{16}$ running along the *b*-axis. It is found from the picture that three InO_n polyhedra form short chains that interconnected by isolated PO_4 groups. In order to make clear inspection, we take a short chain in Fig. 6. It contains three typical In atoms: In1, In2 and In3. The In2 atoms are decahedrally coordinated by seven oxygen atoms while the In1 and In3 atoms are both octahedrally coordinated by six oxygen atoms. In2 decahedron is edge-shared with In1 octahedron, whereas the In1 octahedron is corner-shared with In3 group. The In–O bond distances in In1 polyhedron range from 2.063(2) to 2.217(2) Å, and the In2–O bond distances vary from 2.087(3) to 2.388(3) Å, the In–O bond distances in In3 group lie between 2.078(3) and 2.225(2) Å. This indicates all the InO_n polyhedra are slightly distorted.

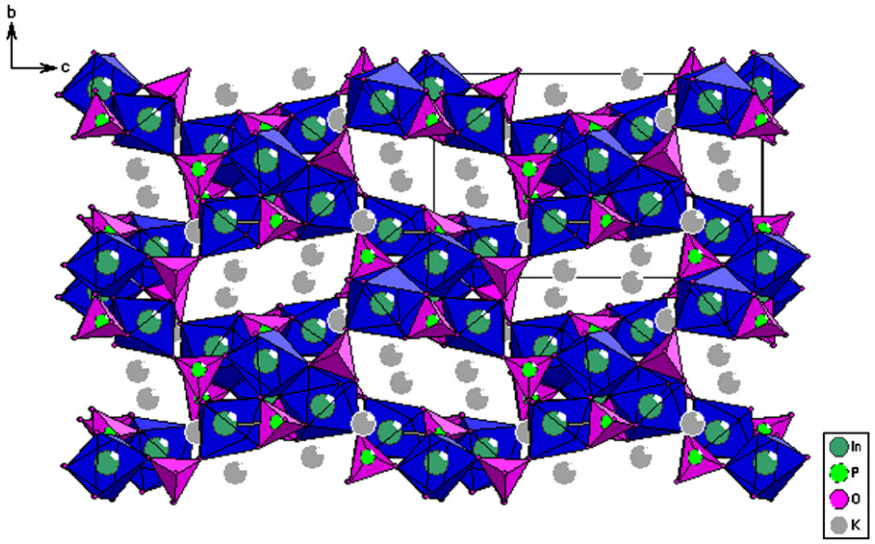

Fig. 2. The framework of $K_3In_3P_4O_{16}$ along the *a*-axis (the pink is PO_4 groups and the blue is InO_n polyhedra). For interpretation of the references to color in this figure legend, the reader is referred to the web version of this article.

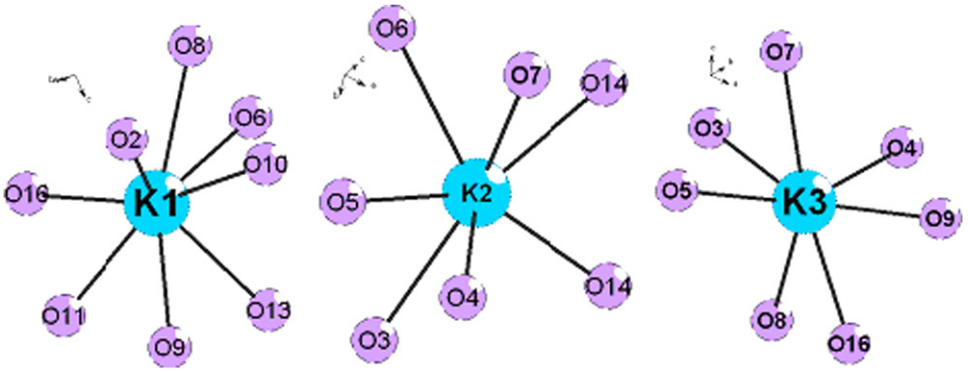

Fig. 3. The local coordination geometries of K cations in $K_3In_3P_4O_{16}$.

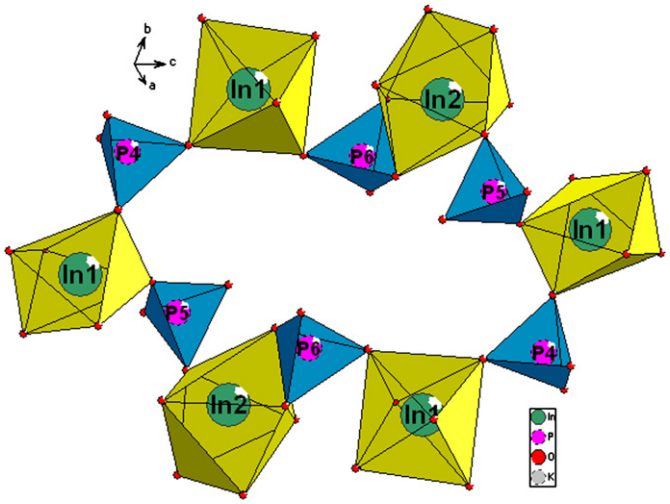

Fig. 4. View of the 12-membered ring composed of alternatively connected InO_n polyhedra and $[PO_4]$ tetrahedra.

Differing from the PO_4 groups in $K_3In(PO_4)_2$ [15,16], the PO_4 tetrahedra in $K_3In_3P_4O_{16}$ are also isolated, but have four types: P4, P5, P6, P7. As shown in Fig. 5, the P4 tetrahedron is corner-shared with two In1 octahedra, one In2 decahedron and one In3 octahedron, respectively, and the P–O bond distances were distorted from 1.515(3) to 1.535(3) Å. By sharing one edge, the P5 group is connected to one In2 decahedron, and then one In3 octahedron is linked to this tetrahedron via a terminal of this sharing edge, other two apices of the P5 group are connected to another In2 and In1 polyhedra, respectively. The P–O bond distances range from 1.521(3) to 1.552(3) Å due to the different environment. The P6 tetrahedron is similar to the P5 tetrahedron, one In2 decahedron is edge-shared with the group, then In3 octahedron is connected to one terminal of this edge, whereas In3 and In1 polyhedra are linked to other two apices of P6 group. The P–O bond distances vary from 1.524(3) to 1.565(2) Å. The P7 tetrahedron is edge-shared with one In1 octahedron, and then one In3 octahedron is linked to a terminal of this edge, other two apices are connected to one In3 and one In2 polyhedra. The P–O bond distances are from 1.516(3) to 1.575(2) Å.

3.2. Band structure and DOS

The energy band structure of $K_3In_3P_4O_{16}$ has been calculated by the DFT method. As shown in Fig. 7, the valence bands are very flat, and the conduction bands have some oscillations. The lowest energy of conduction band is located at G point, and

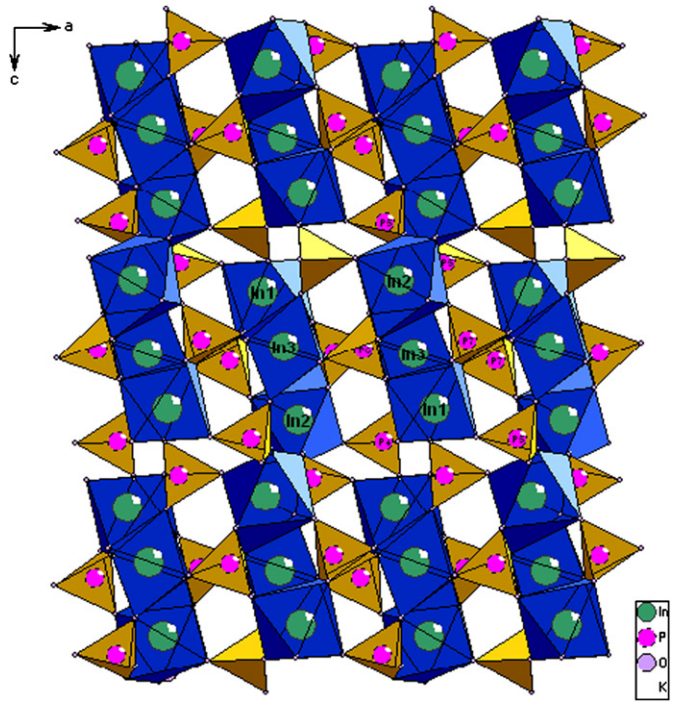

Fig. 5. The structure of $K_3In_3P_4O_{16}$ along the *b*-axis (K^+ is invisible for clarity, the pink is PO_4 groups). For interpretation of the references to color in this figure legend, the reader is referred to the web version of this article.

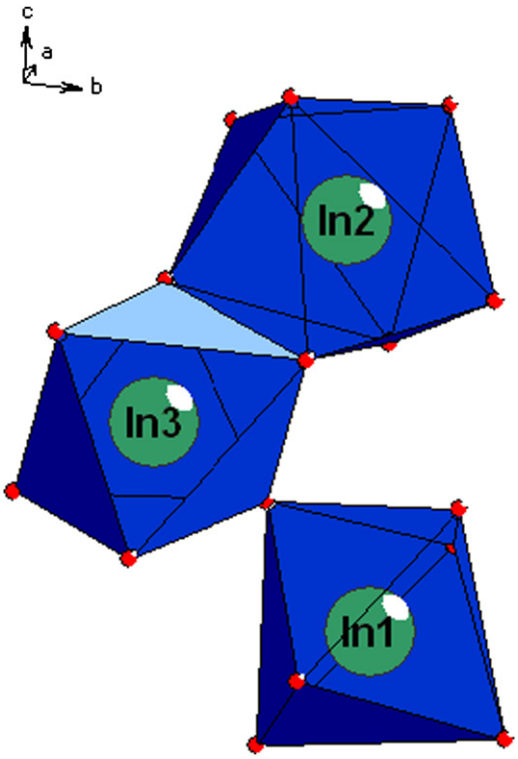

Fig. 6. A short chain of InO_n polyhedron.

the $K_3In_3P_4O_{16}$ shows an isolator with a direct band gap of around 3.01 eV. The bands can be assigned according to total and partial DOS, as shown in Fig. 8. The valence bands near −27.0 and

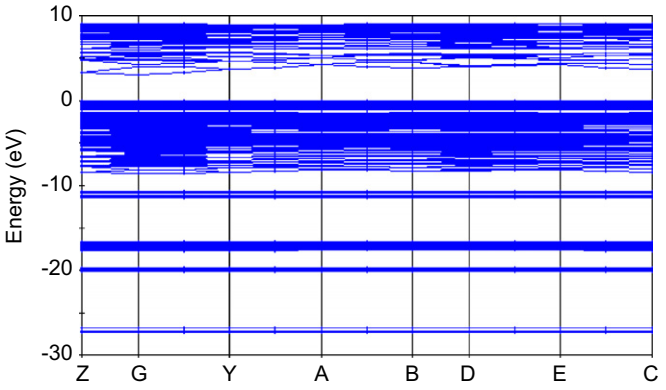

Fig. 7. The energy band structure.

−11.1 eV are almost resulting from the K-4*s* and K-4*p* states. The valence bands located near −20.0 eV are mostly derived from the O-2*s* and P-3*s* states and with small mixings of In-5*p* states. The O-2*s* and P-3*p* states make main contributions to the valence bands near −18.0 and −16.0 eV. The valence bands lying about between −8.5 eV and the Fermi level (0.0 eV) are most formed by the O-2*p* and P-3*p* states with a few mixings of In-5*s*, 5*p* states. The band of the nearest Fermi level is mostly originated from the O-2*p* states. The conduction bands near 3.01 and 9.5 eV result from the In-5*s*, 5*p* states, P-3*p* states with the mixings of K-4*s*, 4*p* states.

3.3. Optical properties of $K_3In_3P_4O_{16}$

The absorption and emission spectra of $K_3In_3P_4O_{16}$ were illustrated in Fig. 9. The absorption edge around 443 nm (2.80 eV) is close to the calculated band gap (3.01 eV) value. The emission spectrum of $K_3In_3P_4O_{16}$ exhibits a broad emission band at around 468 nm under the excitation of the wavelength at 375 nm.

Furthermore, in order to examine the linear optical response properties of $K_3In_3P_4O_{16}$, we calculated the imaginary part $\varepsilon_2(\omega)$ and the real part $\varepsilon_1(\omega)$ of the frequency-dependent dielectric function without the DFT scissor operator approximation. As shown in Fig. 10, there are absorption peaks localized at about 6.24 eV (199 nm), 6.14 eV (202 nm), in x (or *z*) and *y* polarization directions in the dispersion of the calculated $\varepsilon_2(\omega)$ spectra individually, and the crystal is transparent while the wavelength is larger than 276 nm or photon energy is less than 3.17 eV. The observed ultraviolet edge of cut-off is at about 2.80 eV for polycrystalline power sample as shown in Fig. 9. It is shown that our calculated result is reasonable because of transparent ultraviolet edge of the crystal larger than that of the power. The calculated dielectric constants of static case $\varepsilon_1(0)$ are about 2.2868, 2.2285, and 2.2350 in *x*, *y*, and *z* directions, respectively, and the refractive indexes of n_x, n_y, and n_z are 1.5122, 1.4628, and 1.4950, respectively by the relation of $n^2(0) = \varepsilon(0)$, Comparing with the observed refractive indexes of the other phosphate crystals which are generally range from 1.40 to 1.60 [26], the calculated refractive indexes of $K_3In_3P_4O_{16}$ crystal is reasonable.

TPA coefficients β of $K_3In_3P_4O_{16}$ are calculated by expression of $\beta(\omega) \approx B/(n_0^2 Eg^3)F_2(x)$ induced from two-band model [27]. Where *B* is constant of 14206 in units such that β is in cm/GW and energy gap *Eg* is in eV, n_0 is linear refractive index. The function F_2 is only a function of the ratio of the photon energy $\hbar\omega$ to *Eg* (i.e., $x = \hbar\omega/Eg$). The functional form of F_2 reflects the assumed

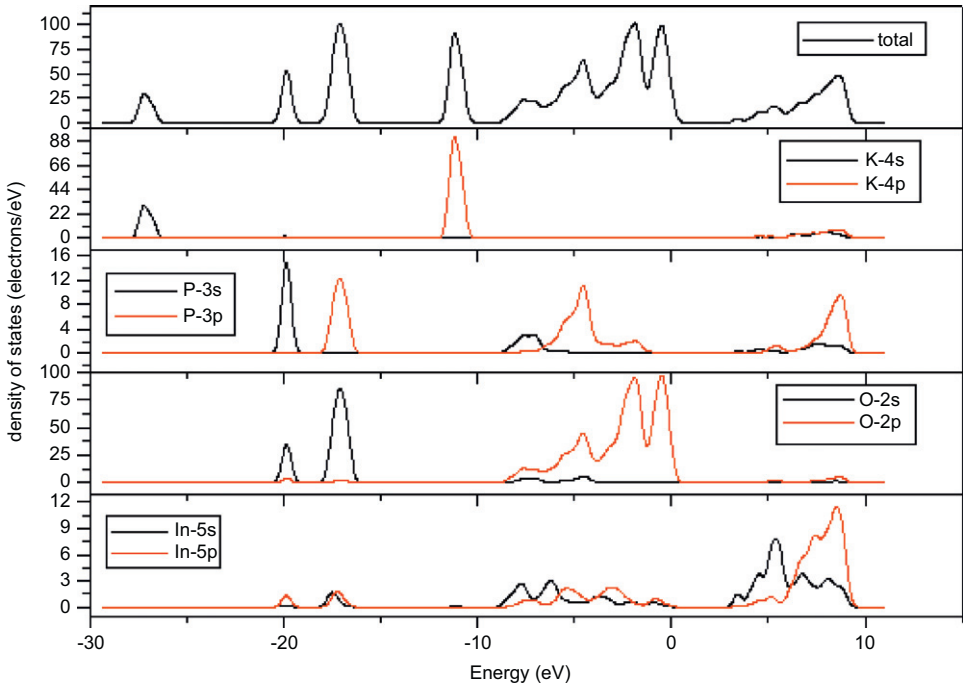

Fig. 8. Density of states of $K_3In_3P_4O_{16}$.

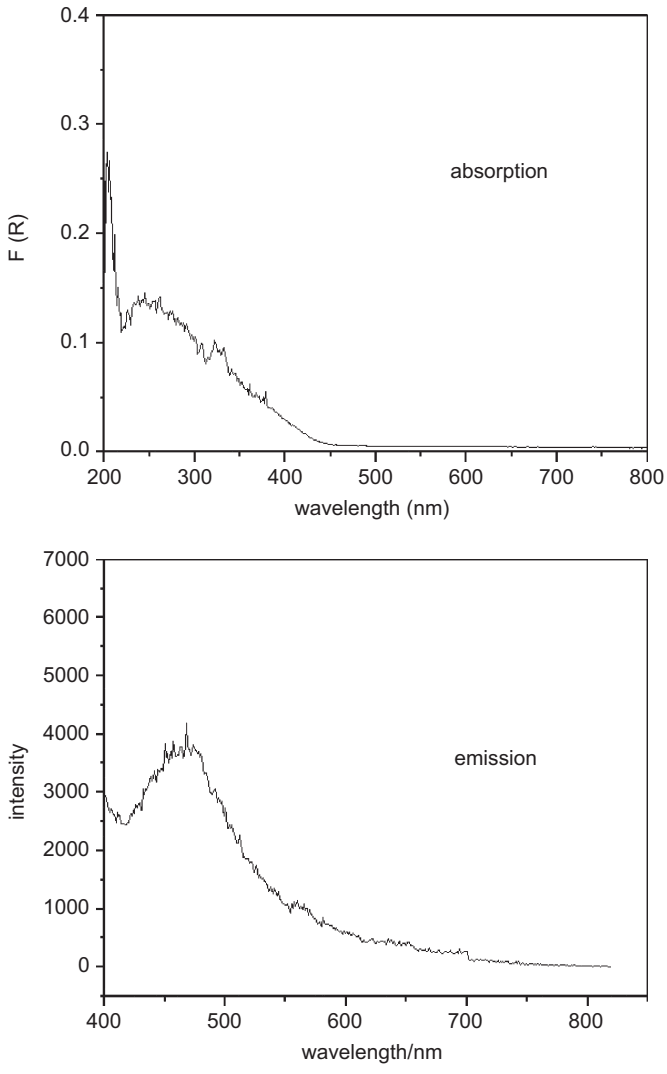

Fig. 9. Absorption and emission spectra of $K_3In_3P_4O_{16}$.

band structure and the intermediate states considered in calculating the TPA transition rate [27] and $F_2(x) = (2x-1)^{3/2}/(2x)^5$ at the same frequency of two incident photons. Fig. 11 shows the calculated TPA spectra of crystal at two-band model. Here, in the calculations of TPA coefficient β, we employ the theoretical Eg value of 3.01 and average linear refractive index n_0 of 1.49. It finds from Fig. 11 that the TPA of $K_3In_3P_4O_{16}$ occurs at energy of larger than 1.50 eV and has the largest TPA coefficient β at 2.10 eV. From the TPA spectra, we predict that the pumping energy of laser fallen within the widow (larger than 1.5 eV) of TPA will lead to optical surface damage of $K_3In_3P_4O_{16}$ crystal.

4. Conclusions

In summary, a new indium phosphate crystal, $K_3In_3P_4O_{16}$, was synthesized by a high-temperature solid-state reaction. It crystallizes in the monoclinic system with space group $P2_1/n$ and possesses three-dimensional $[In_3(PO_4)_4]_n^{3-}$ anionic frameworks with tunnels occupied by K1 and K_2. The observed absorption edge is at about 443 nm, and the emission peak localizes around 468 nm. The calculated band structure shows that $K_3In_3P_4O_{16}$ is an insulator with a direct band gap of 3.01 eV. Additionally, dielectric constants, refractive indexes and TPA coefficient of $K_3In_3P_4O_{16}$ are calculated. The calculated results of optical properties are reasonable by comparing with the experimental data.

Acknowledgments

This investigation was based on work supported by the National Natural Science Foundation of China under Project 20373073, the National Basic Research Program of China (no. 2007CB815307) and the Knowledge Innovation Program of the Chinese Academy of Sciences, and Fujian Key Laboratory of Nanomaterials (no. 2006L2005).

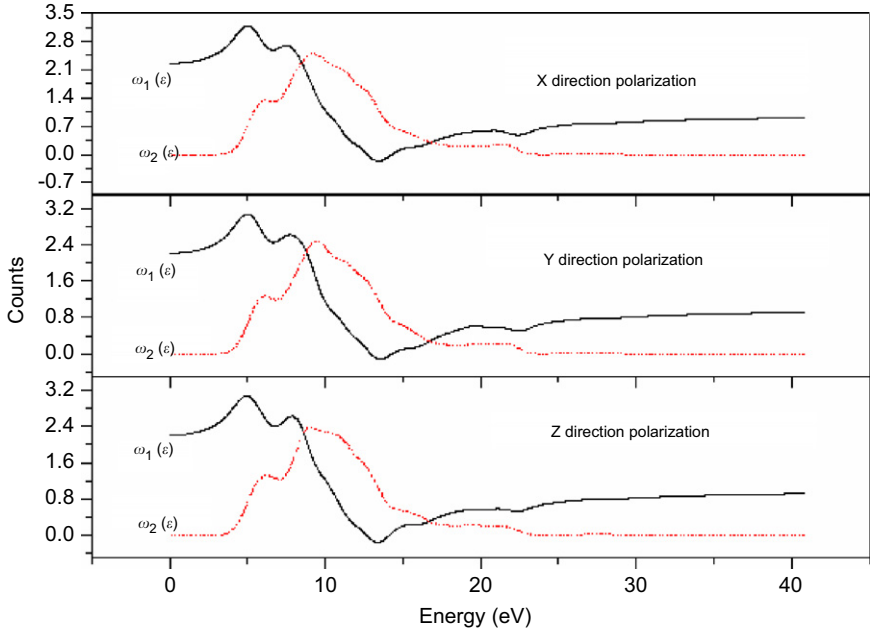

Fig. 10. The calculated dielectric function in different polarization directions.

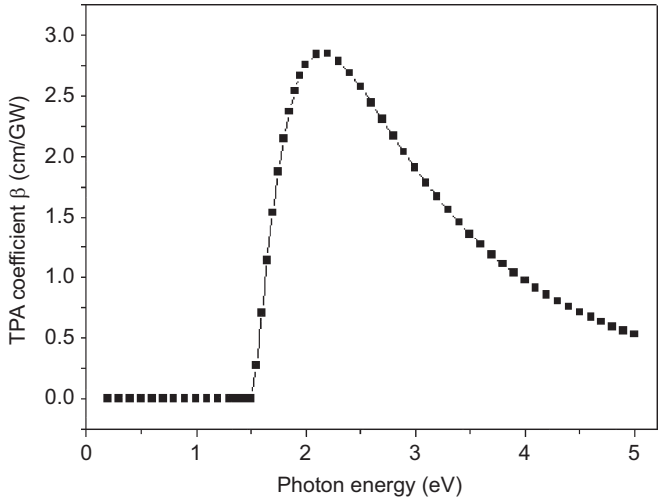

Fig. 11. The calculated two-photon absorption spectra by two-band model.

Appendix A. Supplementary material

Supplementary data associated with this article can be found in the online version at doi:10.1016/j.jssc.2009.01.010.

References

[1] M. Toumi, L. Smiri-Dogguy, A. Bulou, European Journal of Inorganic Chemistry 9 (1999) 1545–1550.
[2] M.A. Strelkov, M.G. Zhizhin, L.N. Komissarova, Journal of Solid State Chemistry 179 (2006) 3664–3671.
[3] Z. Bircsak, W.T.A. Harrison, Acta Crystallographica C 54 (1998) 1554–1556.
[4] M. Ferid, K. Horchani, J. Amami, Materials Research Bulletin 39 (2004) 1949–1955.
[5] D. Riou, N. Nguyen, et al., Materials Research Bulletin 25 (1990) 1363.
[6] R.C. Mercader, L. Terminiello, Physical Review B: Condensed Matter 42 (1990) 25.
[7] A. Guesdon, E. Daguts, B. Raveau, Journal of Solid State Chemistry 167 (2002) 258–264.
[8] I. Belharouak, H. Aouad, M. Mesnaoui, M. Maazaz, Journal of Solid State Chemistry 145 (1999) 97–103.
[9] K. Jaouadi, H. Naili, N. Zouari, T. Mhiri, A. Daoud, Journal of Alloys and Compounds 354 (2003) 104–114.
[10] M.T. Averbuch-Pouchot, Acta Crystallographica C 45 (1989) 1273.
[11] M. Ferid, K. Horchani-Naifer, Materials Research Bulletin 39 (2004) 2209.
[12] I. Parreu, R. Sole, Jna. Gavalda, J. Massons, F. Diaz, M. Aguilo, Chemistry of Materials 15 (2003) 5059–5064.
[13] H. Ettis, H. Naili, T. Mhiri, Crystal Growth & Design 3 (2003) 599–602.
[14] W. Cheng, D.-S. Wu, H. Zhang, D. Chen, Y. Gong, Z. Kan, Chemistry of Materials 16 (2004) 4150.
[15] A.V. Arakcheeva, G. Chapuis, V. Petricek, M. Dusek, A. Schoenleber, Acta Crystallographica B 59 (2003) 17–27.
[16] Y. Zhang, W. Cheng, D. Wu, H. Zhang, D. Chen, Y. Gong, Z. Kan, J. Zhu, Journal of Solid State Chemistry 179 (2006) 186.
[17] H.M. Rietveld, Journal of Applied Crystallography 2 (1969) 65.
[18] Brett Hunter International Union of Crystallography Commission on Powder Diffraction Newsletter no. 20, 1998.
[19] G.M. Sheldirck, SHELXTL, Crystallographic Sotfware Package, SHELXTL, Version 5.1, Bruker-AXS, Madison, WI, 1998.
[20] J.P. Perdew, K. Burke, M. Ernzerhof, Physical Review Letters 77 (1996) 3865.
[21] M. Segall, P. Lindan, M. Probert, C. Pickard, P. Hasnip, S. Clark, M. Payne, Materials Studio CASTEP Version 2.2, Accelrys, Inc., San Diego, CA, 2002.
[22] M.D. Segall, P.L.D. Lindan, M.J. Probert, C.J. Pickard, P.J. Hasnip, S.J. Clark, M.C. Payne, Journal of Physics: Condensed Materials 14 (2002) 2717.
[23] D.R. Hamann, M. Schluter, C. Chiang, Physical Review Letters 43 (1979) 1494.
[24] R.A. Buchanan, H.E. Rast, H.H. Caspers, Journal of Chemical Physics 44 (1966) 4063.
[25] J.R. Macdonald, M.K. Brachman, Reviews of Modern Physics 28 (1956) 383.
[26] J.A. Dean (Ed.), Lange's Handbook of Chemistry, thirteenth ed., McGraw-Hill Book Company, New York, 1985.
[27] S.-B. Mansoor, D.C. Hutchings, D.J. Hagan, E.W. Van Stryland, IEEE Journal of Quantum Electronics 27 (1991) 1296.